HHS Public Access

Author manuscript

Curr Eye Res. Author manuscript; available in PMC 2022 April 01.

Published in final edited form as:

Curr Eye Res. 2021 April ; 46(4): 515–523. doi:10.1080/02713683.2020.1815793.

Prolonged melanopsin-based photoresponses depend in part on RPE65 and cellular retinaldehyde-binding protein (CRALBP)

Krystal R. Harrison[1,3], **Aaron N. Reifler**[2,3], **Andrew P. Chervenak**[2], **Kwoon Y. Wong**[1,2]

[1]Department of Molecular, Cellular, & Developmental Biology, University of Michigan, Ann Arbor, MI, USA

[2]Department of Ophthalmology & Visual Sciences, University of Michigan, Ann Arbor, MI, USA

[3]Equal contributions

Abstract

Purpose: Intrinsically photosensitive retinal ganglion cells (ipRGCs) contain the photopigment melanopsin and can signal light continuously for many hours. Melanopsin is excited when its chromophore *11-cis*-retinal absorbs a photon and becomes *all-trans*-retinal, which must be reisomerized to *11-cis*-retinal to regenerate photoexcitable melanopsin. Due to the great distance separating ipRGCs from the retinal pigment epithelium (RPE) whose retinoid cycle produces *11-cis*-retinal, ipRGCs had been assumed to regenerate all melanopsin molecules autonomously. Surprisingly, we previously found that pharmacologically inhibiting the retinoid cycle rendered melanopsin-based responses to prolonged illumination less sustained, suggesting that the RPE may supply retinoids to help ipRGCs regenerate melanopsin during extended photostimulation. However, the specificity of those drugs is unclear. Here, we reexamined the role of the retinoid cycle, and tested whether the RPE-to-ipRGC transport of retinoids utilizes cellular retinaldehyde-binding protein (CRALBP), present throughout the RPE and Müller glia.

Methods: To measure melanopsin-mediated photoresponses in isolation, all animals were 8- to 12-month-old rod/cone-degenerate mice. We genetically knocked out RPE-specific 65 kDa protein (RPE65), a critical enzyme in the retinoid cycle. We also knocked out the CRALBP gene *rlbp1* mainly in Foxg1-expressing Müller cells. We obtained multielectrode-array recordings from ipRGCs in a novel RPE-attached mouse retina preparation, and imaged pupillary light reflexes *in vivo*.

Results: Melanopsin-based ipRGC responses to prolonged light became less tonic in both knockout lines, and pupillary light reflexes were also less sustained in RPE65-knockout than control mice.

Conclusions: These results confirm that ipRGCs rely partly on the retinoid cycle to continuously regenerate melanopsin during prolonged photostimulation, and suggest that CRALBP in Müller glia likely transports *11-cis*-retinal from the RPE to ipRGCs – this is the first proposed functional role for CRALBP in the inner retina.

Corresponding Author K. Y. Wong: Kellogg Eye Center, 1000 Wall Street, Ann Arbor, MI 48105, USA. kwoon@umich.edu.

Competing interests

None.

Keywords

retinal pigment epithelium; pupillary light reflex; melanopsin; ipRGC; Müller glia

Introduction

Intrinsically photosensitive retinal ganglion cells (ipRGCs) are output neurons of the mammalian retina that drive irradiance-dependent, nonimage-forming visual responses including pupil constriction, melatonin suppression, and circadian photoentrainment. These ganglion-cell photoreceptors contain the photopigment melanopsin and can signal light continuously for many hours[1]. Like the photopigments of rods and cones, melanopsin uses the chromophore *11-cis*-retinal to sense light: photon absorption isomerizes *11-cis*-retinal to *all-trans*-retinal, which then activates the phototransduction cascade[2, 3]. To restore photosensitivity, *all-trans*-retinal must be reisomerized to *11-cis*-retinal. For rods and cones, such reisomerization involves the nearby retinal pigment epithelium (RPE) which contains enzymes mediating the retinoid cycle. Located far from the RPE, ipRGCs possess intrinsic mechanisms for regenerating *11-cis*-retinal[4–6]. Surprisingly, when we used drugs to inhibit the RPE retinoid cycle or poison Müller glia, melanopsin-based ipRGC and pupil responses to prolonged illumination became less sustained, and exogenous *cis*-retinal rescued the deficit, suggesting that the continuous regeneration of light-sensitive melanopsin during extended photostimulation depends partly on retinoids imported from the RPE to ipRGCs via Müller cells[7], perhaps because ipRGCs' endogenous regenerative mechanisms are insufficient.

Our objectives in this study were twofold. First, the specificity of the drugs we used to inhibit the retinoid cycle[7] is not well-understood, so we sought to reexamine the role of this cycle by disrupting it genetically. Second, if the RPE retinoid cycle does contribute to prolonged melanopsin photoresponses, we wanted to test whether the trafficking of retinoids from the RPE to ipRGCs relies on cellular retinaldehyde-binding protein (CRALBP), present throughout the RPE and Müller glia[8]. In order to measure melanopsin photoresponses in isolation, all mice were homozygous for the *rd1* mutation ($pde6b^{rd1/rd1}$) which causes all rods and the vast majority of cones to degenerate[9]. To achieve the first objective of assessing the role of the retinoid cycle, we compared $pde6b^{rd1/rd1}$ mice with $pde6b^{rd1/rd1}$; $rpe65^{rd12/rd12}$ mice which do not express RPE65 (retinal pigment epithelium-specific 65 kDa protein), a critical component of the retinoid cycle[10]; for simplicity we will call them "*rd1; rpe65* control" and "*rd1; rpe65* knockout" mice respectively. To achieve the second objective of testing whether CRALBP traffics retinoids from the RPE through Müller cells to ipRGCs, we aimed to knock out the CRALBP gene, *rlbp1*, in RPE and Müller cells as selectively as possible. Thus we crossed an *rlbp1* flox line with mice expressing Cre recombinase under the *foxg1* promoter which is active in Müller cells[11] and a subset of RPE cells[12], and compared the resulting "*rd1; foxg1::rlbp1* knockout" mice with Cre-negative "*rd1; rlbp1* control" littermates.

Methods

Mouse lines

All procedures were approved by the University of Michigan Institutional Animal Care and Use Committee. All animals were rod/cone-degenerate mice homozygous for the *pde6b*^{rd1} mutation. To produce "*rd1; rpe65* knockout" mice, *rd1* mice homozygous for the *pde6b*^{rd1} mutation were crossed with mice homozygous for the *rpe65*^{rd12} mutation to create heterozygous offspring, which were then intercrossed and genotyped using the primer sets "rd1 seq For-Rev" and "rd12 seq For-Rev" (Table 1), producing *pde6b*$^{rd1/rd1}$*; rpe65*$^{rd12/rd12}$ mice, with *pde6b*$^{rd1/rd1}$*; rpe65*$^{+/+}$ littermates serving as "*rd1; rpe65* control".

To produce "*rd1; foxg1::rlbp1* knockout" mice, we obtained mice containing the *rlbp1*$^{tm1a(EUCOMM)Wtsi}$ allele ("rlbp1-A" in Fig. 1A) from the European Conditional Mouse Mutagenesis Program[13]. They were mated with FLPo transgenic mice[14] that had been backcrossed to C57BL/6 mice, in order to remove the DNA sequences flanked by the FRT sites to produce the conditional allele "rlbp1-B" that carries *rlbp1* exon 5 flanked by loxP sites (Fig 1A). These resulting pups were genotyped to verify the presence of the floxed *rlbp1* (*rlbp1*^{B}) gene. The animals containing *rlbp1-B* were crossed with *pde6b*$^{rd1/rdd1}$ mice over two generations to produce *pde6b*$^{rd1/rd1}$*; rlbp1*$^{B/B}$, which were then crossed with a Cre recombinase line, *foxg1*$^{Cre/+}$, over two generations to obtain *pde6b*$^{rd1/rd1}$*; rlbp1*$^{B/B}$*; foxg1*$^{Cre/+}$ breeders. The *pde6b*$^{rd1/rd1}$*; rlbp1*$^{B/B}$*; foxg1*$^{Cre/+}$ progeny mice ("*rd1; foxg1::rlbp1* knockout") were compared with Cre-negative *pde6b*$^{rd1/rd1}$*; rlbp1*$^{B/B}$*; foxg1*$^{+/+}$ littermates ("*rd1; rlbp1* control"). We did not use *pde6b*$^{rd1/rd1}$*; rlbp1*$^{+/+}$*; foxg1*$^{Cre/+}$ mice as control because *rlbp1*$^{B/B}$ and *rlbp1*$^{+/+}$ might not be functionally equivalent. Table 1 lists all genotyping primers.

In *pde6b*$^{rd1/rd1}$ mice, rod degeneration is complete by postnatal day 65, although a small percentage of cone nuclei (but not outer segments) survive beyond 4 months of age[9]. The residual cone nuclei in 6–10-week-old *pde6b*$^{rd1/rd1}$ mice appear incapable of driving pupillary light reflexes because when melanopsin was knocked out in these mice to block ipRGC photoreception, such reflexes were abolished[15]. Our experiments used mice between 8 and 12 months old, of both sexes.

Immunohistochemistry

Each mouse was dark-adapted overnight and euthanized using CO_2 followed by cervical dislocation. Eyecups were harvested under dim red light in PBS or Ames' medium (MilliporeSigma, St. Louis MO). After 1 hr fixation in 4% paraformaldehyde, each eyecup was rinsed three times in PBS, and infiltrated with increasing concentrations of sucrose at 4 °C: 10% sucrose in PBS for 30 min, 20% sucrose in PBS for 30 min, and 30% sucrose in PBS for 30 min. The eyecup was then incubated in a 2:1 mix of 30% sucrose/PBS and Tissue-Tek optimum cutting temperature compound for 1 hr at room temperature, frozen using dry ice, and kept in a −70 °C freezer for long-term storage. After allowing the tissue block to equilibrate to a cryostat's temperature, it was sectioned at 15 μm thickness. The sections were placed on Superfrost glass slides and allowed to dry for 10 min. After using an ImmEdge pen to draw a hydrophobic barrier around each sectioned tissue, we incubated the

tissue in primary block (PBS containing 10% normal donkey serum and 0.5% Triton X-100) at room temperature for 2 hr, and then in primary block plus a mouse anti-CRALBP antibody diluted 1:1000 (MilliporeSigma catalog no. MA1–813) overnight at 4 °C. The slides were rinsed three times using PBS, and incubated in secondary block (PBS with 5% normal donkey serum and 0.5% Triton X-100) plus donkey anti-mouse secondary antibody tagged with either FITC or Cy5 (Jackson Immuno; 1:250) for 30 min at room temperature. After rinsing the slides three times using PBS, the sections were submerged in Fluoromount-G mounting medium (SouthernBiotech, Birmingham AL) and covered with cover slips. Immunofluorescence was imaged using the 488 nm or 633 nm laser of a Leica SP5 confocal microscope.

Multielectrode-array (MEA) extracellular spike recording

Each mouse was dark-adapted for 15–20 hr. Under dim red light, it was euthanized using CO_2 followed by cervical dislocation, and one eye was harvested and submerged in room-temperature Ames' medium gassed with 95% O_2 5% CO_2. Under infrared night vision goggles, an eyecup was generated and its peripheral parts gently cut away by a razor blade, leaving an approximately 2.2 mm × 2.2 mm square containing the optic disc at the center; the vitreous was left intact, as vitrectomy could detach the retina from the RPE. In the experiment using RPE-detached retinas, the RPE was gently removed from the retina using forceps, and the isolated retina was also cut into an approximately 2.2 mm × 2.2 mm square containing the optic disc at the center, with the vitreous left intact. For both RPE-attached and RPE-detached retinas, the preparation was flattened ganglion cell side down onto a 60-channel MEA with 30μm electrodes at 200μm spacing (Multi Channel Systems, Germany) and anchored by a weighted nylon mesh. Thirty-three °C Ames' medium containing 16 mM D-glucose was fed into the MEA chamber at 4–5 mL min^{-1} and recycled using a peristaltic pump, and continuously gassed by 95% O_2 5% CO_2 in the MEA chamber as well as the reservoir. We chose not to include synaptic blockers so that the MEA recordings and *in vivo* pupillometry were conducted under relatively similar conditions, and because synaptic blockers might alter photoresponse sustainedness by changing the membrane potentials of ipRGCs[16]. After superfusion in darkness for 2 hr, a full-field 480 nm light produced by a monochromator (Optical Building Blocks, Birmingham NJ) was presented continuously from below the MEA for 60 min (Figs. 2A and 4A, *stimulus trace*), with 14.6 log photons cm^{-2} s^{-1} intensity at the retina.

We only analyzed photoresponses lasting >2 min as cells exhibiting shorter responses could have been unhealthy. Spike clustering was performed using Offline Sorter software (Plexon, Dallas TX). Spike histograms were generated in Origin software (OriginLab, Northampton MA) with 1-min bins (Figs. 2B and 4B) and the tallest column (always the first column during the 60-min stimulus) was used to calculate the peak response (Figs. 2C and 4C, *left plot*); specifically, the average of the 2 pre-stimulus columns (reflecting spontaneous spiking) was subtracted from the tallest column. Photoresponse sustainedness was quantified at the midpoint and near the end of the stimulus: *1*) the "30min-to-peak ratio" (Figs. 2C and 4C, *middle plot*) was calculated by subtracting the average of the 2 pre-stimulus columns from the average of the 29^{th} and 30^{th} columns during the stimulus, and dividing this difference by the peak response; *2*) the "60min-to-peak ratio" (Figs. 2C and 4C, *right plot*)

was calculated by subtracting the average of the 2 pre-stimulus columns from the average of the 59th and 60th columns during the stimulus, and dividing this difference by the peak response. For both ratios, a higher value would indicate a more sustained photoresponse. The 30min-to-peak ratio allows a direct comparison of the ipRGC responses with the pupil responses, which were evoked using a 30-min light step (see below). Statistical comparisons were made between *rd1; rpe65* control and *rd1; rpe65* knockout, and between *rd1; rlbp1* control and *rd1; foxg1::rlbp1* knockout, using unpaired Student's *t*-test for normally distributed data and Mann-Whitney *U* test for non-normal data, with $p < 0.05$ indicating a significant difference.

Pupillary light reflex (PLR) imaging

Animals were handled as previously described[17]. Briefly, each dark-adapted mouse was i.p. injected with the sedative acepromazine (5 mg/kg; VetOne, Boise ID), and anesthesia induced by 4% isoflurane. Then it was placed on a recirculating water blanket set at 41 °C, and the isoflurane level reduced to 0.5%. The right pupil was dilated by 2.5% phenylephrine hydrochloride (Paragon BioTeck, Portland OR) and 1% tropicamide (Akorn, Lake Forest IL). The left pupil was kept moist by Goniovisc hypromellose lubricating gel (HUB Pharmaceuticals, Rancho Cucamonga CA) and imaged continuously using an EyeLink 1000 Plus eye tracker (SR Research, Ottawa ON, Canada) first in darkness for 1 min, and then 470 nm LED light (16.0 log photons cm^{-2} s^{-1}) was presented continuously to the right eye for 30 min (Figs. 3A and 5A, *stimulus trace*), shorter than the MEA stimulus duration because in PLR sessions the amount of glare often increased over time due to drifts of the lubricating gel, making it difficult to image for >30 min. Right after imaging, the mouse was euthanized by CO_2 and cervical dislocation.

Pupil diameters were measured offline using a custom LabVIEW program[17]. To generate Figs. 3B and 5B, the pre-stimulus pupil diameters were averaged and normalized to 1, and all subsequent diameters were expressed as fractions of this normalized baseline. To calculate the peak response (Figs. 3C and 5C, *left plot*), the minimum pupil diameter during the stimulus was subtracted from the averaged pre-stimulus diameter, and this difference was divided by the averaged pre-stimulus diameter. To quantify response sustainability, we calculated the "final-to-peak ratio" (Figs. 3C and 5C, *right plot*) by subtracting the average of the pupil diameters during the final 2 min of the stimulus from the averaged pre-stimulus diameter, and dividing this difference by the difference between the averaged pre-stimulus diameter and the minimum diameter (i.e. the peak response); a higher ratio would indicate a more sustained PLR. Statistics were performed as described above for the MEA data.

Results

Functional deficits in *rd1; rpe65* knockout ipRGCs and mice

To investigate whether eliminating RPE65 would compromise melanopsin-based photoresponses in ipRGCs, we used the MEA to record action potentials from 78 *rd1; rpe65* control ipRGCs (from 8 mice) and 70 *rd1; rpe65* knockout ipRGCs (from 6 mice) in RPE-attached retinas. Though diverse photoresponse durations were seen within each genotype, responses lasting throughout the 60-min light were somewhat more common in *rd1; rpe65*

control ipRGCs than in their knockout counterparts, and Fig. 2A (*top* and *middle recordings*) provides representative examples. Indeed, the population-averaged spike histograms (Fig. 2B *left* and *middle plots*) show that although both genotypes' photoresponses decayed over time, the mean spike rate of *rd1; rpe65* control cells stayed above the baseline throughout the 60-min light, whereas the knockout cells' mean spike rate had fully returned to the baseline by the end of that light. Confirming that this *ex vivo* retinal preparation preserves retina-RPE connectivity, ipRGCs in RPE-detached *rd1; rpe65* control retinas gave photoresponses that fully returned to the baseline well before the end of the 60-min light (Figs. 2A *bottom recording*, 2B *right plot*), far more transient than the photoresponses from RPE-attached *rd1;rpe65* control retinas (Figs. 2A *top recording*, 2B *left plot*). Statistical comparisons of *rd1; rpe65* control and knockout ipRGC photoresponses (recorded from RPE-attached retinas) are summarized in Fig. 2C. The two genotypes had statistically similar peak response spike rates near the beginning of the 60-min light (Mann-Whitney $p = 0.072$; *left plot*), but the 30min-to-peak and 60min-to-peak response ratios were both significantly higher in the *rd1; rpe65* control (Mann-Whitney $p = 0.0085$ and 0.0099 respectively; *middle and right plots*), confirming that the absence of RPE65 accelerated the decay of the melanopsin photoresponse during the light step.

To ascertain whether abolishing RPE65 expression would impact melanopsin-mediated nonimage-forming visual behavior, we measured PLRs in 20 *rd1; rpe65* control mice and 22 *rd1; rpe65* knockout mice. Fig. 3A shows representative images from two mice, at three time points: just before the 30-min light; peak constriction shortly after light onset; and near the end of this light. The population-averaged pupil diameter measurements (Fig. 3B) suggest that while the two genotypes had comparable peak responses shortly after stimulus onset, the amount of constriction near the end of the stimulus seemed greater in the control. Statistical comparisons of *rd1; rpe65* control and knockout mice (Fig. 3C) confirm that peak constriction near the beginning of the 30-min light was statistically similar (*t*-test $p = 0.51$; *left plot*), whereas the final-to-peak constriction ratio was significantly higher for *rd1; rpe65* control (*t*-test $p = 0.023$; *right plot*), indicating that RPE65 helps sustain the melanopsin-based PLR during the 30-min light step.

Functional deficits in *rd1; foxg1::rlbp1* knockout ipRGCs and mice

Having established that the RPE retinoid cycle helps sustain melanopsin-based responses to prolonged illumination, we next examined whether such sustainability depends on CRALBP in the RPE and/or Müller glia, by knocking out the floxed *rlbp1* gene using *foxg1*-driven Cre recombinase (Fig. 1A). Within the retina, *foxg1*-driven Cre expression is restricted to Müller glia[11]. CRALBP immunostaining was virtually eliminated within the neural retina, suggesting that Müller cells no longer contained this protein, although staining was still visible in the RPE (Fig. 1B *right*), presumably reflecting CRALBP in non-Foxg1-expressing RPE cells[12]. No obvious staining remained when the immunohistochemistry protocol omitted the primary antibody (not shown).

We first recorded from 45 *rd1; rlbp1* control ipRGCs (from 9 mice) and 136 *rd1; foxg1::rlbp1* knockout ipRGCs (from 13 mice) and measured their spiking responses to the 60-min light step. The control cells had a tendency to exhibit longer-lasting responses than

the knockout cells, as illustrated in the example recordings (Fig. 4A) and the population-averaged spike histograms (Fig. 4B). Statistical comparisons (Fig. 4C) confirm that *rd1; rlbp1* control ipRGCs had more sustained photoresponses than *rd1; foxg1::rlbp1* knockout ipRGCs, as the former had significantly higher 30min- and 60min-to-peak response ratios (Mann-Whitney $p = <0.00001$ and 0.0080 respectively; *middle and right plots*), although the two genotypes had comparable peak responses (*t*-test $p = 0.36$; *left plot*).

Finally we imaged 30-min PLRs in 9 *rd1; rlbp1* control mice and 20 *rd1; foxg1::rlbp1* knockout mice, and Fig. 5A shows example data. The averaged responses in Fig. 5B suggest that the two genotypes had comparable peak responses, while constriction near the end of the stimulus seemed stronger in the control. However, even though the difference in the mean final-to-peak constriction ratio was sizeable (Fig. 5C *right plot*), this difference was not statistically significant (*t*-test $p = 0.16$), which could conceivably be a type II error caused by the relatively small sample ($n = 9$) of the *rd1; rlbp1* control; limited resources precluded the generation of more mice.

Discussion

We have developed a novel MEA recording preparation that preserves mouse retina-RPE connectivity. In earlier studies[1, 7] we successfully obtained RPE-attached rat retinas from eyecup pieces lacking the optic disc, but when equivalent pieces of mouse eyecups were flattened onto the MEA, the RPE detached from the retina easily, and few ipRGCs could give hour-long photoresponses. In the present study, we overcame this limitation by using a piece of mouse eyecup containing the optic disc which helped keep the retina attached to the RPE.

We previously[7] inhibited the retinoid cycle pharmacologically using *13-cis*-retinoic acid[18] and α-phenyl-*N*-tert-butylnitrone[19], but here we knocked out *rpe65* genetically. The two approaches have different pros and cons: the drugs acted acutely but potentially had off-target effects, while gene knockout was specific but could have induced developmental changes[20, 21]. Nonetheless, these divergent approaches gave the same result, namely, disrupting the retinoid cycle made melanopsin-based responses to 14.6 log photons cm^{-2} s^{-1} 480 nm light less tonic, thus strengthening the hypothesis that the RPE helps regenerate melanopsin during extended photostimulation, presumably to complement ipRGCs' intrinsic regenerative mechanism(s) such as photoreversal[6]. A 2006 paper reported that *rpe65*$^{+/-}$ and *rpe65*$^{-/-}$ rodless mice gave similar circadian phase shift responses, but it only tested a low-intensity 15min-duration stimulus[4]. In Zhao *et al.* 2016 we showed that melanopsin's dependence on the retinoid cycle could only be detected if the stimulus was sufficiently intense and prolonged, i.e. 14.6 log photons cm^{-2} s^{-1} for >5 min and 12.8 log photons cm^{-2} s^{-1} for >25 min. In the current study, *rd1* mice with and without RPE65 gave comparable melanopsin-based responses shortly after stimulus onset, but as light stimulation continued the knockout mice's responses became progressively weaker than the control's, so that the knockout mice had significantly lower 30min-to-peak response ratios.

Although knocking out *rpe65* in rodless mice had modest to no impact on short-duration melanopsin photoresponses[4, 5], such photoresponses were drastically reduced when *rpe65*

was knocked out in mice with structurally intact photoreceptors[3–5]. A plausible explanation is that the photoreceptors compete with ipRGCs for the small amounts of chromophores present in RPE65-deficient retinas[22], and eliminating most of the photoreceptors allows ipRGCs better access to these chromophores[4, 5]. The dramatically suppressed melanopsin photoresponses in such *rpe65* knockout mice would have made it difficult to study the sustainedness of these photoresponses. Thus, in the present study we opted to knock out *rpe65* in rod/cone-degenerate mice, in order to better preserve melanopsin photoresponses.

We have also investigated a potential mechanism for trafficking retinoids from the RPE to ipRGCs. Two proteins are known to shuttle retinoids within the RPE at different steps of the retinoid cycle: cellular retinol binding protein (CRBP) binds to *all-trans*-retinol, and CRALBP binds to *11-cis*-retinol and *11-cis*-retinal[23–25]. CRALBP in RPE cells' apical processes may also serve to export *11-cis*-retinal to the subretinal space[26]. Moreover, CRALBP is present in Müller cells and has been proposed to facilitate the release of *11-cis*-retinol to cones, which then isomerize it to *11-cis*-retinal[27]. Knocking out the CRALBP gene *rlbp1* delayed rods' and cones' dark adaptation and attenuated their photoresponses[27, 28]. Before the current study, one prior study had tested for a contribution of CRALBP to ipRGC photoreception by comparing the PLRs of *rlbp1*$^{-/-}$ and control mice at high light intensities (up to 15.5 log photons cm^{-2} s^{-1}), and no difference was found; however, stimulus duration was only 30 sec, and only peak response amplitudes were analyzed[27]. By increasing stimulus duration to 30 min (for PLRs) and 60 min (for MEA recordings), we found that while knocking out *rlbp1* in Foxg1-expressing cells (i.e. Müller glia and some RPE cells) did not affect peak response amplitudes, it significantly reduced response sustainedness. In both *rd1; foxg1::rlbp1* and *rd1; rpe65* knockouts, the deficits appeared more pronounced for the MEA recordings than for the PLRs (compare the 30min-to-peak ratios in Figs. 2C, 4C with the final-to-peak ratios in Figs. 3C, 5C), as previously observed in rats[7]. Considering that the MEA recordings likely included multiple ipRGC types[29, 30] whereas the PLRs reflected mainly the M1 type[31], a plausible explanation is that RPE65 and CRALBP are more important for non-M1 than M1 ipRGCs. The various ipRGC types' diverse photoresponse kinetics[32] may also have contributed to the sizable SEMs for the 30min-to-peak and 60min-to-peak ratios of the MEA-recorded light responses (Figs. 2C, 4C).

Immunostaining of *rd1; foxg1::rlbp1* knockout eye sections revealed robust CRALBP expression in the RPE, but virtually no expression in the neural retina and hence Müller cells. (In fact, CRALBP staining in the RPE of these mice seemed even stronger than that in control mice, although immunohistochemistry is not a quantitative assay.) Since Foxg1 is expressed in a mosaic of RPE cells[12], the overall CRALBP level in the RPE probably decreased in *rd1; foxg1::rlbp1* knockout mice, so the photoresponse deficits seen in these mice could be caused by the lack of CRALBP in Müller cells, or the presumed reduced expression of this protein in the RPE, or both. We suspect these deficits were caused mainly (though not exclusively) by the lack of CRALBP in Müller cells, not just because the *foxg1*-dependent *rlbp1* knockout impacted these glia more than the RPE, but also because it is unlikely that reduced expression (as opposed to elimination) of this protein in the RPE would cause a phenotype as severe as that for *rd1; rpe65* knockout mice, whose retinas have undetectable levels of *11-cis*-retinal[10] – compare Figs. 2B *middle* and 4B *right*. Thus, we hypothesize that the *rd1; foxg1::rlbp1* knockout phenotype is caused mainly by an inability

of Müller cells to transport retinoids from the RPE to ipRGCs, essentially blocking ipRGCs' access to exogenous retinoids. This hypothesis is appealing because CRALBP is abundantly present throughout Müller cells, from the outer limiting membrane to the inner limiting membrane[8], but the only function demonstrated so far is exporting *11-cis*-retinol to cones in the outer retina[27], and so the presence of CRALBP in the inner retina remained a mystery.

How might ipRGCs receive retinoids from the RPE? Interphotoreceptor retinoid-binding protein (IRBP) could traffic retinoids from the RPE to Müller cells[8], in which CRALBP could subsequently shuttle them toward ipRGCs. CRALBP can bind to both *11-cis*-retinal and *11-cis*-retinol[25], so theoretically it could transport both *11-cis*-retinal from the RPE retinoid cycle and *11-cis*-retinol from Müller cells' cone-specific cycle[23], but since ipRGCs cannot utilize *11-cis*-retinol to regenerate melanopsin[7, 33] and CRALBP has a higher affinity for *11-cis*-retinal than *11-cis*-retinol[34], we propose that CRALBP transports *11-cis*-retinal to ipRGCs.

Besides obtaining retinoids from the RPE, melanopsin regeneration during photostimulation also involves photoreversal where *all-trans*-retinal remains linked to a photoexcited melanopsin molecule, and subsequent photon absorption isomerizes it to *11-cis*-retinal thereby making the melanopsin molecule photoexcitable again[6]. Additional mechanisms probably contribute to melanopsin regeneration, because our observation that the peak responses at light onset were similar in *rd1; rpe65* knockout and control mice (Figs. 2C *left*, 3C *left*) indicates that full melanopsin regeneration had occurred during the preceding dark period despite the lack of photoreversal (which requires light exposure) and RPE65. Several retinoid-processing enzymes have been identified in Müller glia and the ganglion cell layer, e.g. dihydroceramide desaturase-1 (DES1)[35], multifunctional O-acyltransferase (MFAT)[36], diacylglycerol O-acyltransferase-1 (DGAT1)[37], and retinal G-protein-coupled receptor (RGR)[38]. These enzymes could produce chromophores for ipRGCs and/or cones, but probably not rods since rod photosensitivity is abolished in RPE65-deficient mice[39].

rlbp1 mutations can cause various human eye diseases such as autosomal recessive retinitis pigmentosa[40], Bothnia dystrophy[41], retinitis punctate albescens[42], and fundus albipunctatus[43]. Severe impairments in rod/cone function are well documented[44–46]. Our results suggest that these diseases could potentially also impact ipRGC photoreception and hence nonimage-forming visual responses such as circadian photoentrainment, melatonin suppression, and mood regulation.

Acknowledgments

This work was funded by NIH NEI grants EY023660 and EY007003, and an Alliance for Vision Research grant.

References

1. Wong KY. A retinal ganglion cell that can signal irradiance continuously for 10 hours. J Neurosci 2012:32(33): 11478–11485. [PubMed: 22895730]
2. Walker MT, Brown RL, Cronin TW, Robinson PR. Photochemistry of retinal chromophore in mouse melanopsin. Proc Natl Acad Sci U S A 2008:105(26): 8861–8865. [PubMed: 18579788]

3. Fu Y, Zhong H, Wang MH, Luo DG, Liao HW, Maeda H, Hattar S, Frishman LJ, Yau KW. Intrinsically photosensitive retinal ganglion cells detect light with a vitamin a-based photopigment, melanopsin. Proc Natl Acad Sci U S A 2005:102(29): 10339–10344. [PubMed: 16014418]

4. Doyle SE, Castrucci AM, McCall M, Provencio I, Menaker M. Nonvisual light responses in the rpe65 knockout mouse: Rod loss restores sensitivity to the melanopsin system. Proc Natl Acad Sci U S A 2006:103(27): 10432–10437. [PubMed: 16788070]

5. Tu DC, Owens LA, Anderson L, Golczak M, Doyle SE, McCall M, Menaker M, Palczewski K, Van Gelder RN. Inner retinal photoreception independent of the visual retinoid cycle. Proc Natl Acad Sci U S A 2006:103(27): 10426–10431. [PubMed: 16788071]

6. Emanuel AJ, Do MT. Melanopsin tristability for sustained and broadband phototransduction. Neuron 2015:85(5): 1043–1055. [PubMed: 25741728]

7. Zhao X, Pack W, Khan NW, Wong KY. Prolonged inner retinal photoreception depends on the visual retinoid cycle. J Neurosci 2016:36(15): 4209–4217. [PubMed: 27076420]

8. Bunt-Milam AH, Saari JC. Immunocytochemical localization of two retinoid-binding proteins in vertebrate retina. J Cell Biol 1983:97(3): 703–712. [PubMed: 6350319]

9. Carter-Dawson LD, LaVail MM, Sidman RL. Differential effect of the rd mutation on rods and cones in the mouse retina. Invest Ophthalmol Vis Sci 1978:17(6): 489–498. [PubMed: 659071]

10. Pang JJ, Chang B, Hawes NL, Hurd RE, Davisson MT, Li J, Noorwez SM, Malhotra R, McDowell JH, Kaushal S et al. Retinal degeneration 12 (rd12): A new, spontaneously arising mouse model for human leber congenital amaurosis (lca). Mol Vis 2005:11(152–162. [PubMed: 15765048]

11. Ivanova E, Hwang GS, Pan ZH. Characterization of transgenic mouse lines expressing cre recombinase in the retina. Neuroscience 2010:165(1): 233–243. [PubMed: 19837136]

12. Pratt T, Tian NM, Simpson TI, Mason JO, Price DJ. The winged helix transcription factor foxg1 facilitates retinal ganglion cell axon crossing of the ventral midline in the mouse. Development 2004:131(15): 3773–3784. [PubMed: 15240555]

13. Consortium I Infrafrontier--providing mutant mouse resources as research tools for the international scientific community. Nucleic Acids Res 2015:43(Database issue): D1171–1175. [PubMed: 25414328]

14. Kranz A, Fu J, Duerschke K, Weidlich S, Naumann R, Stewart AF, Anastassiadis K. An improved flp deleter mouse in c57bl/6 based on flpo recombinase. Genesis 2010:48(8): 512–520. [PubMed: 20506501]

15. Panda S, Provencio I, Tu DC, Pires SS, Rollag MD, Castrucci AM, Pletcher MT, Sato TK, Wiltshire T, Andahazy M et al. Melanopsin is required for non-image-forming photic responses in blind mice. Science 2003:301(5632): 525–527. [PubMed: 12829787]

16. Zhao X, Reifler AN, Schroeder MM, Jaeckel ER, Chervenak AP, Wong KY. Mechanisms creating transient and sustained photoresponses in mammalian retinal ganglion cells. J Gen Physiol 2017:149(3): 335–353. [PubMed: 28153865]

17. Eckley SS, Villano JS, Kuo NS, Wong KY. Acepromazine and chlorpromazine as pharmaceutical-grade alternatives to chlorprothixene for pupillary light reflex imaging in mice. J Am Assoc Lab Anim Sci 2020:59(2): 197–203. [PubMed: 31915106]

18. Sieving PA, Chaudhry P, Kondo M, Provenzano M, Wu D, Carlson TJ, Bush RA, Thompson DA. Inhibition of the visual cycle in vivo by 13-cis retinoic acid protects from light damage and provides a mechanism for night blindness in isotretinoin therapy. Proc Natl Acad Sci U S A 2001:98(4): 1835–1840. [PubMed: 11172037]

19. Mandal MN, Moiseyev GP, Elliott MH, Kasus-Jacobi A, Li X, Chen H, Zheng L, Nikolaeva O, Floyd RA, Ma JX et al. Alpha-phenyl-n-tert-butylnitrone (pbn) prevents light-induced degeneration of the retina by inhibiting rpe65 protein isomerohydrolase activity. J Biol Chem 2011:286(37): 32491–32501. [PubMed: 21785167]

20. Caruso RC, Aleman TS, Cideciyan AV, Roman AJ, Sumaroka A, Mullins CL, Boye SL, Hauswirth WW, Jacobson SG. Retinal disease in rpe65-deficient mice: Comparison to human leber congenital amaurosis due to rpe65 mutations. Invest Ophthalmol Vis Sci 2010:51(10): 5304–5313. [PubMed: 20484585]

21. Tanabu R, Sato K, Monai N, Yamauchi K, Gonome T, Xie Y, Takahashi S, Ishiguro SI, Nakazawa M. The findings of optical coherence tomography of retinal degeneration in relation to the

morphological and electroretinographic features in rpe65−/− mice. PLoS One 2019:14(1): e0210439. [PubMed: 30695025]

22. Fan J, Rohrer B, Moiseyev G, Ma JX, Crouch RK. Isorhodopsin rather than rhodopsin mediates rod function in rpe65 knock-out mice. Proc Natl Acad Sci U S A 2003:100(23): 13662–13667. [PubMed: 14578454]
23. Wang JS, Kefalov VJ. The cone-specific visual cycle. Prog Retin Eye Res 2011:30(2): 115–128. [PubMed: 21111842]
24. Napoli JL. A gene knockout corroborates the integral function of cellular retinol-binding protein in retinoid metabolism. Nutr Rev 2000:58(8): 230–236. [PubMed: 10946560]
25. Saari JC, Bredberg L, Garwin GG. Identification of the endogenous retinoids associated with three cellular retinoid-binding proteins from bovine retina and retinal pigment epithelium. J Biol Chem 1982:257(22): 13329–13333. [PubMed: 6292186]
26. Nawrot M, West K, Huang J, Possin DE, Bretscher A, Crabb JW, Saari JC. Cellular retinaldehyde-binding protein interacts with erm-binding phosphoprotein 50 in retinal pigment epithelium. Invest Ophthalmol Vis Sci 2004:45(2): 393–401. [PubMed: 14744877]
27. Xue Y, Shen SQ, Jui J, Rupp AC, Byrne LC, Hattar S, Flannery JG, Corbo JC, Kefalov VJ. Cralbp supports the mammalian retinal visual cycle and cone vision. J Clin Invest 2015:125(2): 727–738. [PubMed: 25607845]
28. Saari JC, Nawrot M, Kennedy BN, Garwin GG, Hurley JB, Huang J, Possin DE, Crabb JW. Visual cycle impairment in cellular retinaldehyde binding protein (cralbp) knockout mice results in delayed dark adaptation. Neuron 2001:29(3): 739–748. [PubMed: 11301032]
29. Tu DC, Zhang D, Demas J, Slutsky EB, Provencio I, Holy TE, Van Gelder RN. Physiologic diversity and development of intrinsically photosensitive retinal ganglion cells. Neuron 2005:48(6): 987–999. [PubMed: 16364902]
30. Walch OJ, Zhang LS, Reifler AN, Dolikian ME, Forger DB, Wong KY. Characterizing and modeling the intrinsic light response of rat ganglion-cell photoreceptors. J Neurophysiol 2015:114(5): 2955–2966. [PubMed: 26400257]
31. Guler AD, Ecker JL, Lall GS, Haq S, Altimus CM, Liao HW, Barnard AR, Cahill H, Badea TC, Zhao H et al. Melanopsin cells are the principal conduits for rod-cone input to non-image-forming vision. Nature 2008:453(7191): 102–105. [PubMed: 18432195]
32. Zhao X, Stafford BK, Godin AL, King WM, Wong KY. Photoresponse diversity among the five types of intrinsically photosensitive retinal ganglion cells. J Physiol 2014:592(7): 1619–1636. [PubMed: 24396062]
33. Sexton TJ, Golczak M, Palczewski K, Van Gelder RN. Melanopsin is highly resistant to light and chemical bleaching in vivo. J Biol Chem 2012:287(25): 20888–20897. [PubMed: 22547062]
34. Golovleva I, Bhattacharya S, Wu Z, Shaw N, Yang Y, Andrabi K, West KA, Burstedt MS, Forsman K, Holmgren G et al. Disease-causing mutations in the cellular retinaldehyde binding protein tighten and abolish ligand interactions. J Biol Chem 2003:278(14): 12397–12402. [PubMed: 12536144]
35. Kaylor JJ, Yuan Q, Cook J, Sarfare S, Makshanoff J, Miu A, Kim A, Kim P, Habib S, Roybal CN et al. Identification of des1 as a vitamin a isomerase in muller glial cells of the retina. Nat Chem Biol 2013:9(1): 30–36. [PubMed: 23143414]
36. Kaylor JJ, Cook JD, Makshanoff J, Bischoff N, Yong J, Travis GH. Identification of the 11-cis-specific retinyl-ester synthase in retinal muller cells as multifunctional o-acyltransferase (mfat). Proc Natl Acad Sci U S A 2014:111(20): 7302–7307. [PubMed: 24799687]
37. Kaylor JJ, Radu RA, Bischoff N, Makshanoff J, Hu J, Lloyd M, Eddington S, Bianconi T, Bok D, Travis GH. Diacylglycerol o-acyltransferase type-1 synthesizes retinyl esters in the retina and retinal pigment epithelium. PLoS One 2015:10(5): e0125921. [PubMed: 25974161]
38. Diaz NM, Morera LP, Tempesti T, Guido ME. The visual cycle in the inner retina of chicken and the involvement of retinal g-protein-coupled receptor (rgr). Mol Neurobiol 2017:54(4): 2507–2517. [PubMed: 26984602]
39. Redmond TM, Yu S, Lee E, Bok D, Hamasaki D, Chen N, Goletz P, Ma JX, Crouch RK, Pfeifer K. Rpe65 is necessary for production of 11-cis-vitamin a in the retinal visual cycle. Nat Genet 1998:20(4): 344–351. [PubMed: 9843205]

40. Maw MA, Kennedy B, Knight A, Bridges R, Roth KE, Mani EJ, Mukkadan JK, Nancarrow D, Crabb JW, Denton MJ. Mutation of the gene encoding cellular retinaldehyde-binding protein in autosomal recessive retinitis pigmentosa. Nat Genet 1997:17(2): 198–200. [PubMed: 9326942]

41. Burstedt MS, Forsman-Semb K, Golovleva I, Janunger T, Wachtmeister L, Sandgren O. Ocular phenotype of bothnia dystrophy, an autosomal recessive retinitis pigmentosa associated with an r234w mutation in the rlbp1 gene. Arch Ophthalmol 2001:119(2): 260–267. [PubMed: 11176989]

42. Fishman GA, Roberts MF, Derlacki DJ, Grimsby JL, Yamamoto H, Sharon D, Nishiguchi KM, Dryja TP. Novel mutations in the cellular retinaldehyde-binding protein gene (rlbp1) associated with retinitis punctata albescens: Evidence of interfamilial genetic heterogeneity and fundus changes in heterozygotes. Arch Ophthalmol 2004:122(1): 70–75. [PubMed: 14718298]

43. Katsanis N, Shroyer NF, Lewis RA, Cavender JC, Al-Rajhi AA, Jabak M, Lupski JR. Fundus albipunctatus and retinitis punctata albescens in a pedigree with an r150q mutation in rlbp1. Clin Genet 2001:59(6): 424–429. [PubMed: 11453974]

44. Granse L, Abrahamson M, Ponjavic V, Andreasson S. Electrophysiological findings in two young patients with bothnia dystrophy and a mutation in the rlbp1 gene. Ophthalmic Genet 2001:22(2): 97–105. [PubMed: 11449319]

45. Hipp S, Zobor G, Glockle N, Mohr J, Kohl S, Zrenner E, Weisschuh N, Zobor D. Phenotype variations of retinal dystrophies caused by mutations in the rlbp1 gene. Acta Ophthalmol 2015:93(4): e281–286. [PubMed: 25429852]

46. Burstedt MS, Sandgren O, Golovleva I, Wachtmeister L. Effects of prolonged dark adaptation in patients with retinitis pigmentosa of bothnia type: An electrophysiological study. Doc Ophthalmol 2008:116(3): 193–205. [PubMed: 17922155]

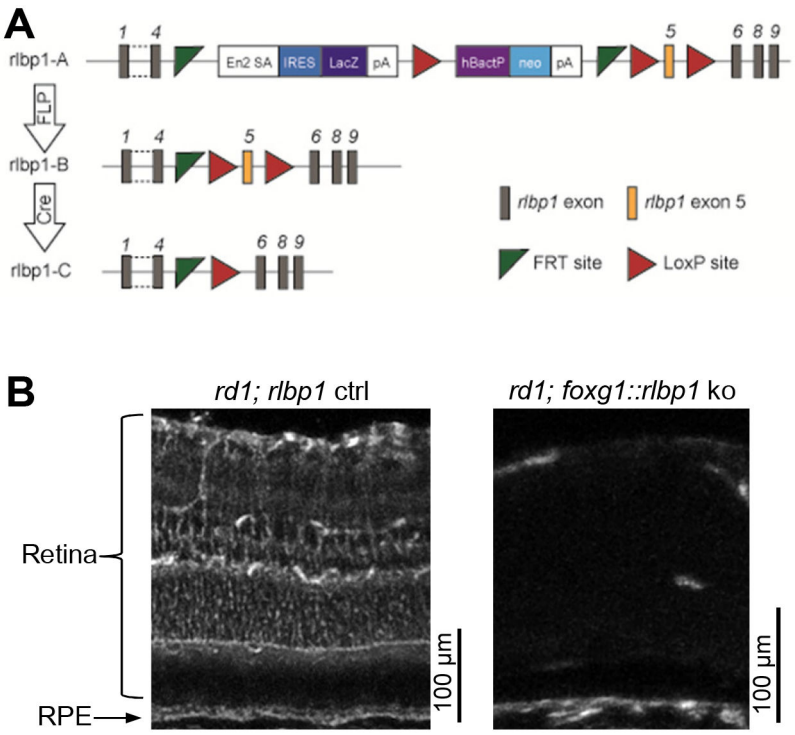

Fig. 1.

Creating *rd1; foxg1::rlbp1* knockout mice and characterizing CRALBP expression. *A*) The creation of *pde6b*$^{rd1/rd1}$*; rlbp1*$^{B/B}$*; foxg1*$^{+/+}$ ("*rd1; rlbp1* control") and *pde6b*$^{rd1/rd1}$*; rlbp1*$^{B/B}$*; foxg1*$^{Cre/+}$ ("*rd1; foxg1::rlbp1* knockout") mice. "rlbp1-A" mice were mated with FLPo mice to produce "rlbp1-B" mice. After crossing the latter with *pde6b*$^{rd1/rd1}$ mice, the resulting *pde6b*^{rd1}*; rlbp1*^{B} mice were mated with a *foxg1*^{Cre} line to produce "rlbp1-C" mice in which the *rlbp1* exon 5 was excised in Foxg1-expressing cells. Cre-negative littermates served as controls. *B*) CRALBP immunostaining in posterior eye sections. In *rd1; rlbp1* control mice (*left*) prominent CRALBP expression was detected in both retina and RPE. By contrast, in *rd1; foxg1::rlbp1* knockout mice (*right*) CRALBP staining was nearly absent in the retina.

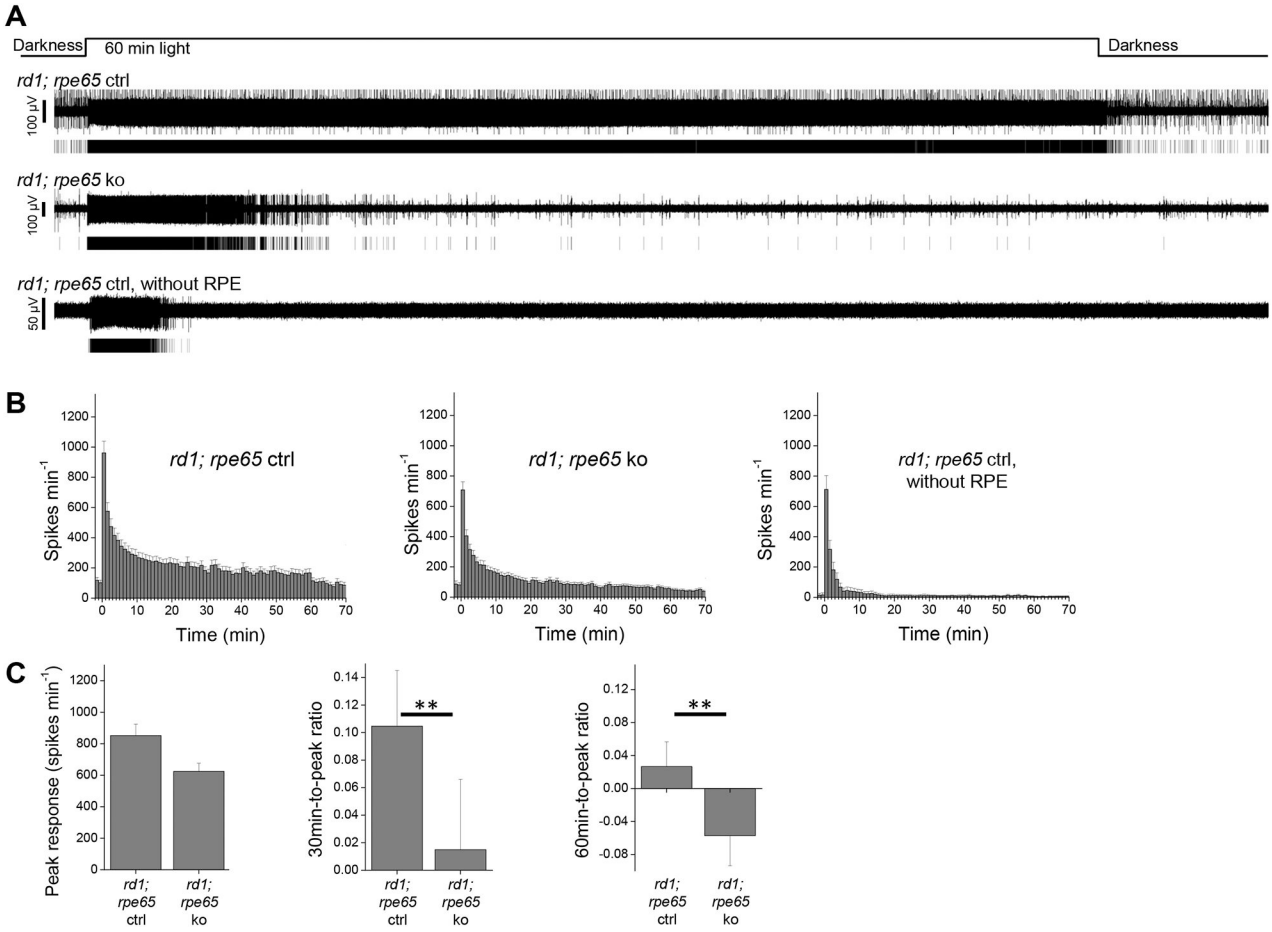

Fig. 2.

Multielectrode-array (MEA) recordings of *pde6b*$^{rd1/rd1}$*; rpe65*$^{+/+}$ ("*rd1; rpe65* control") and *pde6b*$^{rd1/rd1}$*; rpe65*$^{rd12/rd12}$ ("*rd1; rpe65* knockout") ipRGCs. *A*) The photostimulation protocol (*top trace*) and representative raw recordings from three ipRGCs, with the corresponding raster plot underneath each recording. The top and middle recordings were made from RPE-attached *rd1; rpe65* control and *rd1; rpe65* knockout retinas respectively, whereas the bottom recording was from an *rd1; rpe65* control retina that had been mechanically isolated from the RPE. The stimulus was full-field 480 nm light at 14.6 log photons cm^{-2} s^{-1}. *B*) Spike histograms averaged from all *rd1; rpe65* control ipRGCs (n = 78) and *rd1; rpe65* knockout ipRGCs (n = 70) in RPE-attached retinas, and all *rd1; rpe65* control ipRGCs (n = 33) in RPE-detached retinas. *C*) Comparisons of photoresponse features between the two genotypes, based on the MEA recordings from RPE-attached retinas. From left to right: the peak light-evoked spike rate near the beginning of the 60-min light step; 30min-to-peak ratio of the photoresponse; and 60min-to-peak ratio of the photoresponse. Error bars are S.E.M. **, $p < 0.01$.

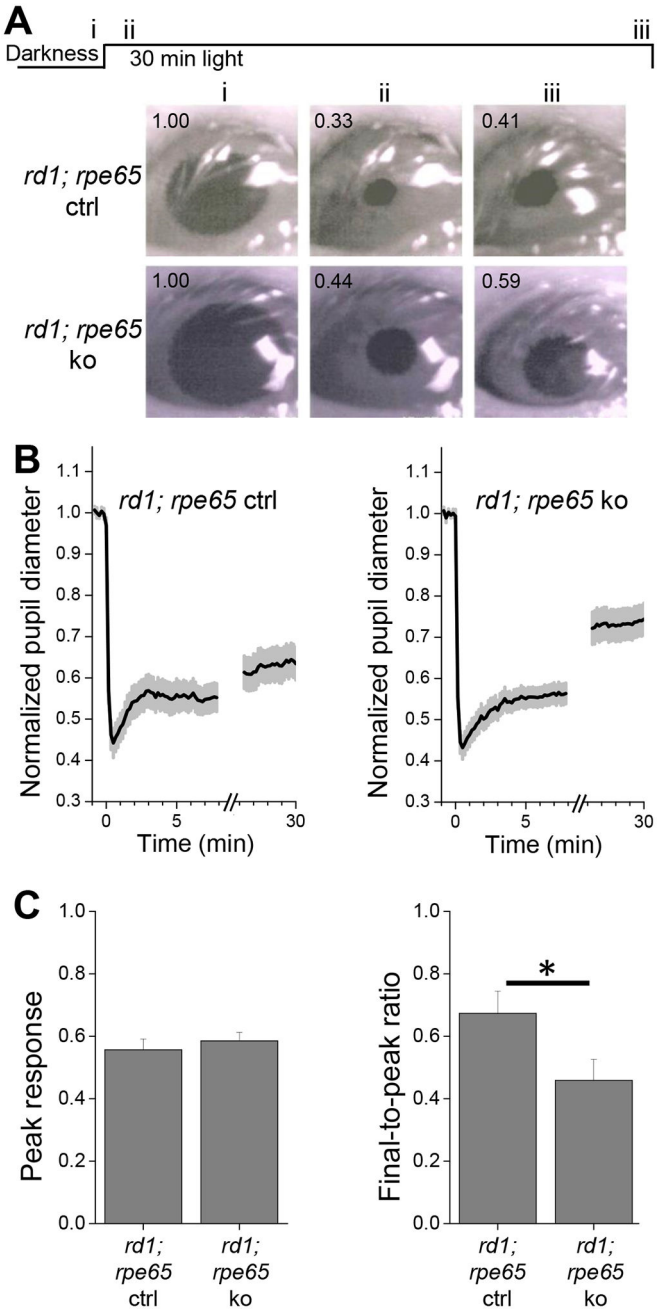

Fig. 3.

Pupillary light reflexes (PLRs) of *rd1; rpe65* control and *rd1; rpe65* knockout mice. *A*) The photostimulation protocol (*top trace*) and representative images from two mice. The Roman numerals above the protocol trace indicate the three time points for the example images, and the numbers within the images are normalized pupil diameters. The stimulus was full-field 470 nm light at 16.0 log photons cm^{-2} s^{-1}. *B*) Pupil diameters averaged from all *rd1; rpe65* control mice ($n = 20$) and *rd1; rpe65* knockout mice ($n = 22$) during the first 9 min of imaging including 1 min of pre-stimulus darkness, and the last ~4 min of the 30-min light step. The black traces depict mean diameters and the surrounding gray areas depict S.E.M.

C) Comparisons of the *rd1; rpe65* control and *rd1; rpe65* knockout PLRs. *Left*: Peak pupil constriction during the 30-min light step. *Right*: Final-to-peak constriction ratio during that light step. Error bars are S.E.M. *, $p < 0.05$.

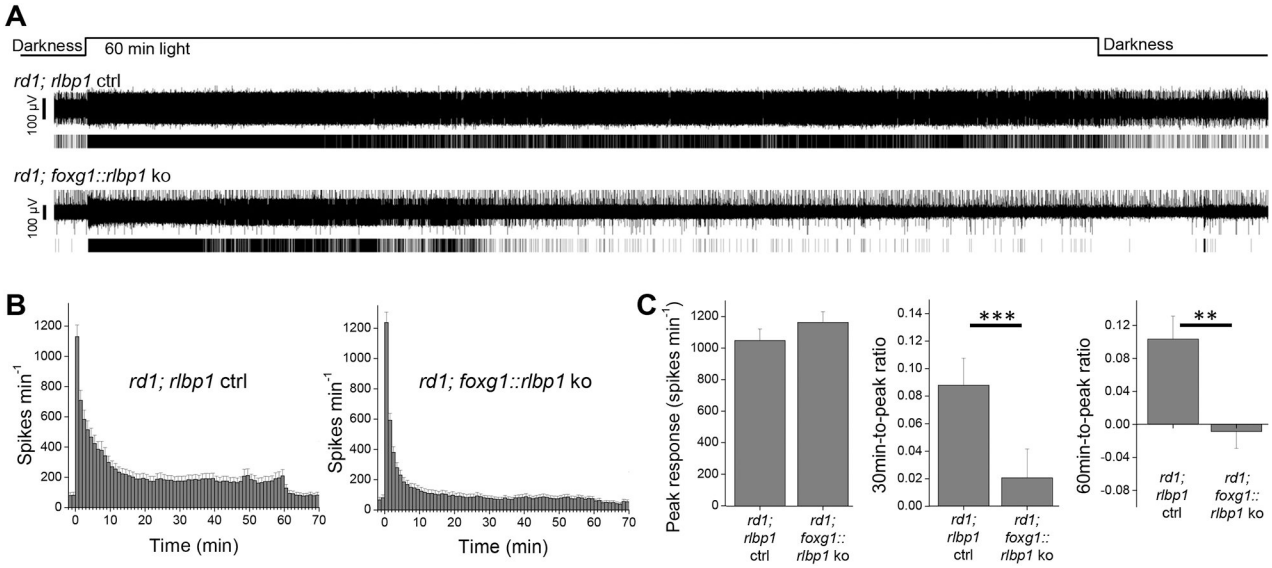

Fig. 4.

MEA recordings of *pde6b*$^{rd1/rd1}$*; rlbp1*$^{B/B}$*; foxg1*$^{+/+}$ ("*rd1; rlbp1* control") and *pde6b*$^{rd1/rd1}$*; rlbp1*$^{B/B}$*; foxg1*$^{Cre/+}$ ("*rd1; foxg1::rlbp1* knockout") ipRGCs. *A*) The photostimulation protocol, representative raw recordings from two ipRGCs in RPE-attached retinas, and corresponding raster plots. *B*) Spike histograms averaged from all *rd1; rlbp1* control ipRGCs (n = 45) and *rd1; foxg1::rlbp1* knockout ipRGCs (n = 136). *C*) Comparisons of the two genotypes' photoresponses. Error bars are S.E.M. **, $p < 0.01$. ***, $p < 0.001$.

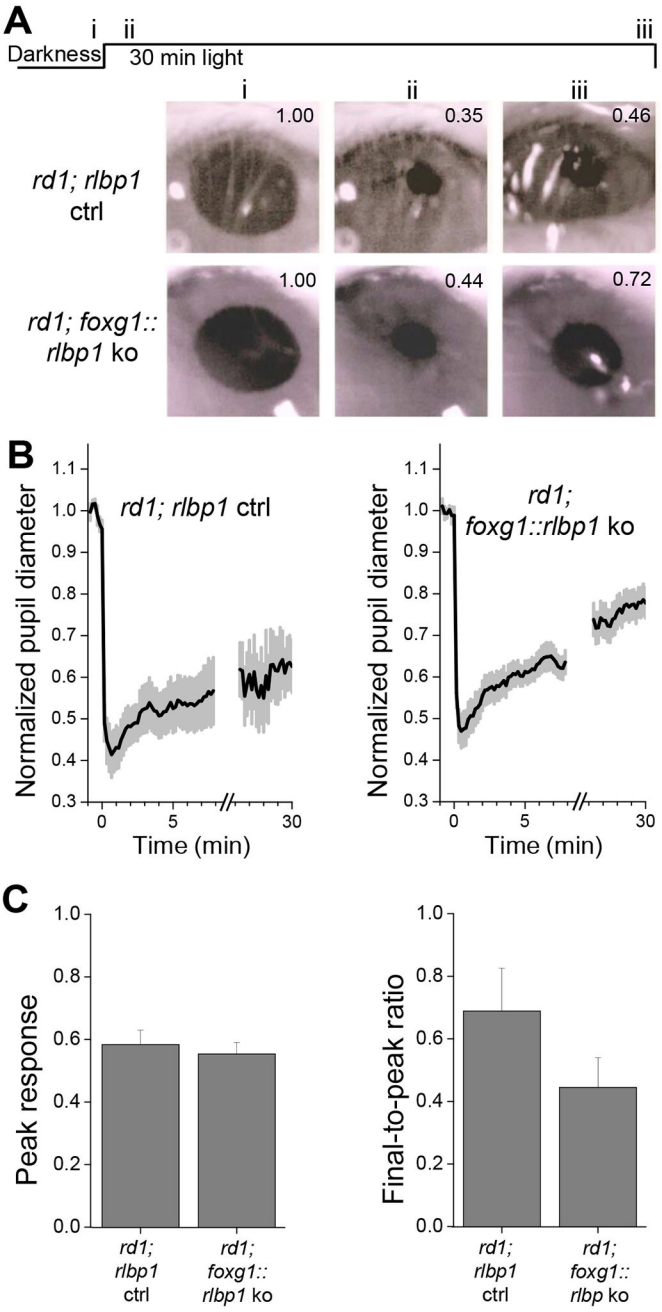

Fig. 5.

PLRs of *rd1; rlbp1* control and *rd1; foxg1::rlbp1* knockout mice. *A*) The photostimulation protocol and representative images from two mice, with the numbers inside the images indicating normalized pupil diameters. *B*) Pupil diameters averaged from all *rd1; rlbp1* control mice ($n = 9$) and *rd1; foxg1::rlbp1* knockout mice ($n = 20$). *C*) Comparisons of the *rd1; rlbp1* control and *rd1; foxg1::rlbp1* knockout PLRs. Error bars are S.E.M.

Table 1

Primers for genotyping.

rd1 seq For	TCCTCATCAGCTTCCTAGCCT
rd1 seq Rev	GGTAGGCAGATTACCTGAAAGT
rd12 seq For	GATCCATGCTCCTAAAGTCTATCC
rd12 seq Rev	GGTGATAGAAAGGCTCAGATCC
rlbp1 5arm F2	CCCTCACTGTGGTTCATAACT
rlbp1 3crit R1	CATGCGTACTGTGCTTTTAC
5’CAS-F1	AAGGCGCATAACGATACCAC
3’LOXP-R1	ACTGATGGCGAGCTCAGACC
Cre_F1	CGACCAGGTTCGTTCACTCA
Cre_R1	CAGCGTTTTCGTTCTGCCAA